

## Acceleration of raindrops formation due to tangling-clustering instability in turbulent stratified atmosphere

T. Elperin<sup>1, a)</sup> N. Kleorin<sup>1, b)</sup> B. Krasovitov<sup>1</sup>, M. Kulmala<sup>2</sup>, M. Liberman<sup>3,4, c)</sup>  
I. Rogachevskii<sup>1, d)</sup> and S. Zilitinkevich<sup>2,5,6</sup>

<sup>1</sup> *The Pearlstone Center for Aeronautical Engineering Studies,  
Department of Mechanical Engineering, Ben-Gurion University  
of the Negev, P. O. Box 653, Beer-Sheva 84105, Israel*

<sup>2</sup> *Division of Atmospheric Sciences, Department of Physics,  
P.O. Box 64, 00014 University of Helsinki, Finland*

<sup>3</sup> *Nordita, KTH Royal Institute of Technology and Stockholm University,  
Roslagstullsbacken 23, 10691 Stockholm, Sweden*

<sup>4</sup> *Moscow Institute of Physics and Technology, Dolgoprudnyi, 141700, Russia*

<sup>5</sup> *Finnish Meteorological Institute (FMI) PO Box 503, 00101 Helsinki, Finland*

<sup>6</sup> *Department of Radio Physics, N. I. Lobachevsky State University of Nizhny  
Novgorod, Russia*

(Dated: 13 April 2019)

Condensation of water vapor on active cloud condensation nuclei produces micron-size water droplets. To form rain, they must grow rapidly into at least 50-100  $\mu\text{m}$  droplets. Observations show that this process takes only 15-20 minutes. The unexplained physical mechanism of such fast growth, is crucial for understanding and modeling of rain, and known as "condensation-coalescence bottleneck in rain formation". We show that the recently discovered phenomenon of the tangling clustering instability of small droplets in temperature-stratified turbulence (Phys. Fluids 25, 085104, 2013) results in the formation of droplet clusters with drastically increased droplet number densities. The mechanism of tangling clustering instability is much more effective than the previously considered pure inertial clustering caused by the centrifugal effect of turbulent vortices. This is the reason of strong enhancement of the collision-coalescence rate inside the clusters. Our analysis of the droplet growth explains the observed fast growth of cloud droplets in warm clouds from the initial 1  $\mu\text{m}$  size droplets to 40-50  $\mu\text{m}$  size droplets within 15-20 minutes.

PACS numbers: 47.27.tb, 47.27.T-, 47.55.Hd

---

<sup>a)</sup>Electronic mail: [elperin@bgu.ac.il](mailto:elperin@bgu.ac.il); <http://www.bgu.ac.il/me/staff/tov>

<sup>b)</sup>Electronic mail: [nat@bgu.ac.il](mailto:nat@bgu.ac.il)

<sup>c)</sup>Electronic mail: [misha.liberman@gmail.com](mailto:misha.liberman@gmail.com); <http://michael-liberman.com/>

<sup>d)</sup>Electronic mail: [gary@bgu.ac.il](mailto:gary@bgu.ac.il); <http://www.bgu.ac.il/~gary>

## I. INTRODUCTION

When ascending parcel of moist air reaches the condensation level, the initial mist of small, micron-size water droplets is formed, which are suspended in the air. In the super-saturated environment water droplets grow due to condensation of water vapor from the surrounding atmosphere. However, to form the raindrops, which can fall down triggering rain, they must grow up to about  $50 \mu\text{m}$  size droplets, which would take a very long time. Observations indicate that the average time for rainfall initiation is approximately  $15 - 20$  minutes, while existing theories predict that the duration of a time interval, required for droplets to grow up to  $50 \mu\text{m}$  in radius, is of the order of hours (see, e.g., reviews 1–3, and references therein). Indeed, though the actual time of large droplets formation depends on the initial droplet size spectrum and cloud water content (see, e.g., Ref. 4), the predicted growth time differs considerably from the observations.

Initiation of rain in turbulent clouds comprises three stages. The first stage involves condensation of water vapor on cloud condensation nuclei (CCN, typically having a size of the order of  $0.05 \mu\text{m}$ ) and formation of small micron size droplets. At the next stage, droplets grow efficiently through condensation and diffusion of water vapor and may attain radii of about  $10 \mu\text{m}$ . It is generally believed that droplets having radii larger than  $50 \mu\text{m}$  fall out of the cloud due to gravitational sedimentation and continue to grow in size mainly through gravitational collisions into rain droplets with the size of the order of  $80 - 100 \mu\text{m}$ . Understanding a mechanism of rapid growth of initially small droplets to the size of the order of  $50 \mu\text{m}$  when gravitational collision-coalescence becomes effective is still poorly understood and remains a subject of active research (see Refs. 1–3). Identifying mechanisms of rapid growth of cloud droplets and determining the growth rate, i.e. theoretical explanation of the so-called "*size gap or the condensation-coalescence bottleneck in warm rain formation*" (see Ref. 3) is one of the major challenges in cloud physics.

Observations show the existence of strong turbulence in clouds. Different mechanisms have been suggested and different aspects of turbulence effects on the growth of cloud droplets have been considered to explain the rapid formation of rain droplets in clouds (see Ref. 3). These mechanisms involve e.g. effects of giant aerosol particles for faster formation of large cloud droplets, thereby initiating coalescence sooner (see Ref. 5) and droplet spectra broadening under conditions of water vapor supersaturation (see Refs. 6–8).

Numerous theoretical, numerical and experimental studies used different approaches and models to investigate the effects of atmospheric turbulence on growth of cloud droplets by collision-coalescence and formation of rain droplets (see Refs. 1–3, and references therein).

Most of the studies have focused on amplification of the fall velocity of cloud droplets in turbulent atmosphere and turbulence induced increase of the droplet collision kernel. Air turbulence can enhance droplet coalescence rate by increasing the relative velocity of droplets due to differential acceleration and enhance collision kernel of cloud droplets. For example, when the dissipation rate of turbulence is increased from 100 to 400  $\text{cm}^2 \text{s}^{-3}$ , the droplet coalescence rate (between droplets with the sizes 18  $\mu\text{m}$  and 20  $\mu\text{m}$ ) increases by a factor of 3.5 (see Ref. 9). The increase of droplet relative velocity and local accumulation of inertial droplets near the periphery of turbulent eddies due to centrifugal effect, can increase droplet collision rate (see Refs. 1, 9–24). Numerical simulations showed that due to the effect of preferential concentration of inertial particles in turbulent flows their settling rate is about 20% larger than the terminal fall velocity in the quiescent atmosphere (see Refs. 1, 10, 14, 15, 18, 20, 21, and 25). This list of references is obviously not complete because the topic is a subject of intense ongoing research and attracts attention of numerous researchers (see Refs. 2 and 3).

Accurate modeling of droplet collision-coalescence is important because collisions strongly affect droplet size and velocity distributions, and dispersion of droplets (see Ref. 26). Droplet collisions may have numerous outcomes - the droplets might smoothly merge with little deformation, bounce off each other, coalesce following large deformation, or separate after temporarily coalescing. Many of the used droplet interaction models assume that droplet velocities before collisions are not correlated. However, this assumption is violated in turbulent flows. Indeed, small droplets have low inertia and follow almost the same trajectories as fluid particles and, therefore, their pre-collision velocities are strongly correlated with the velocity of a carrying fluid (see Ref. 27). Many of the studies focused on collisions between identical droplets whereby the collision outcome depends on the impact parameter and the ratio of kinetic energy to surface tension. It was demonstrated that size disparity can significantly increase the parameter range over which droplets permanently coalesce (see Ref. 28).

Dynamics and interactions of liquid droplets, their collisions, coalescence and bouncing, become more significant with increase of their size and are encountered in many naturally

occurring phenomena and industrial applications, including rain initiation and combustion. Nevertheless, the collision rate for typical droplet number densities in clouds is too far from being sufficient for their efficient coalescence. The general opinion is that turbulence somehow enhances droplet collision rate and droplet coalescence. However, it still remains unclear and not completely established yet to what extent and how turbulence can affect and control droplet coalescence and rain initiation (see Refs. 2 and 3).

In this paper we explain the fast growth of cloud droplets by collision-coalescence taking into account recently discovered phenomenon of tangling clustering instability of small water droplets in turbulent temperature stratified atmosphere (see Ref. 29). We assume that water droplets coalesce after collisions. However, the ambient mean number density of the droplets is too low, so that their collision-coalescence time is very large. The situation dramatically changes in the presence of tangling clustering instability which results in the formation of clusters with the mean number density of the droplets inside the clusters that by several orders of magnitude exceeds the ambient mean number density of the droplets.

The mechanism of droplet clustering in turbulence is as follows. Due to inertia effects droplets inside turbulent eddies are carried out to the boundary between the eddies by inertial forces. Therefore, water droplets are locally accumulated in the regions with low vorticity and maximum pressure fluctuations (see Ref. 30). Contrary to the inertia induced preferential concentration, the pressure fluctuations in stratified turbulence with a nonzero mean temperature gradient are increased due to additional temperature fluctuations generated by tangling of the mean temperature gradient by velocity fluctuations. This is a reason why clustering of water droplets is much more effective in stratified turbulence (see Refs. 29 and 31) in comparison with a non-stratified turbulence (see Ref. 12).

The tangling clustering instability leads to the formation of clusters, which accumulate surrounding droplets. Since the number density and, correspondingly, the collision-coalescence rate of small droplets inside the clusters drastically increase, the characteristic time of droplet coalescence sharply decreases. Effect of the tangling clustering instability (see Ref. 29) is much stronger than that of the inertial clustering instability (see Ref. 12) in non-stratified isotropic and homogeneous turbulence. The dramatic enhancement of droplet collision-coalescence rate caused by the effect of tangling clustering instability of small droplets, explains the observed fast growth of cloud droplets from the initial  $1\ \mu\text{m}$  size droplets to  $40\text{-}50\ \mu\text{m}$  size droplets within 15-20 minutes.

## II. TANGLING CLUSTERING INSTABILITY

Small cloud droplets with the size of the order of  $1 \mu\text{m}$  have to grow in diameter by a factor 50-100 in order to fall out of the cloud as rain droplets. Initial formation of cloud droplets is associated with an intricate process that allows conversion of water vapor into small liquid water droplets. Droplet formation always requires the presence of aerosols and their activation to cloud droplets, and further growth of droplets via condensation-coalescence. Clearly, the growth of cloud droplets is constrained by their vaporization, and droplet collisions and coalescence may modify the droplet size distribution (see Refs. 32–34).

In the present study we invoke recently discovered phenomenon of tangling clustering instability of droplets in temperature stratified turbulence which causes formation of clusters with the droplet number density inside the clusters by several orders of magnitude larger than the ambient droplet number density (see Ref. 29). The size of the formed clusters is of the order of the Kolmogorov micro-scale length. For the sake of simplicity in this section we assume that vapor condensation produces small droplets of the same size, which then grow due to the collision-induced coalescence. The droplet size distribution is taken into account in the next section.

### A. Governing equations

The theory of the tangling clustering instability in the temperature-stratified turbulence has been developed in Ref. 29. In this section we summarize these theoretical results and explain why the clustering instability is essentially enhanced in the turbulence with large-scale temperature gradient. Equation for the instantaneous number density  $n(t, \mathbf{r})$  of small spherical droplets in a turbulent flow reads:

$$\frac{\partial n}{\partial t} + \nabla \cdot (n \mathbf{v}) = D_m \Delta n - \frac{n - n_0}{\tau_{ev}}, \quad (1)$$

where  $D_m = k_B T / (3\pi\rho\nu d)$  is the coefficient of molecular (Brownian) diffusion of droplets having the diameter  $d$  and the instantaneous velocity  $\mathbf{v}(t, \mathbf{r})$ ,  $\nu$  is the kinematic viscosity,  $T$  and  $\rho$  are the mean air temperature and density,  $k_B$  is the Boltzman constant and  $n_0$  is the equilibrium number density of droplets caused by an external source of droplets. The last term in the right hand side of Eq. (1) describes the change of the droplet number density due to external source of droplets and their disappearance by evaporation. Here for the sake

of simplicity we assumed that the characteristic times of the increase and decrease of the droplet number density are equal to the characteristic evaporation time,  $\tau_{ev}$ . However, this assumptions can be easily relaxed.

The clustering instability of droplets in turbulent flow is determined by fluctuations of the droplet number density,  $n'(t, \mathbf{r}) = n(t, \mathbf{r}) - N(t, \mathbf{r})$ . Equation for the fluctuations is (see Refs. 29 and 31):

$$\frac{\partial n'}{\partial t} + \nabla \cdot (n' \mathbf{v} - \langle n' \mathbf{v} \rangle) - D_m \Delta n' = -(\mathbf{v} \cdot \nabla) N - N \nabla \cdot \mathbf{v} - \frac{n'}{\tau_{ev}}, \quad (2)$$

where  $N = \langle n \rangle$  is the mean droplet number density and the droplet velocity  $\mathbf{v}$  is determined by the equation of motion:

$$\frac{d\mathbf{v}}{dt} = \frac{\mathbf{u} - \mathbf{v}}{\tau_{st}} + \mathbf{g}. \quad (3)$$

Here  $\mathbf{u}(t, \mathbf{x})$  is the fluid velocity,  $\mathbf{g}$  is the gravity acceleration,  $\tau_{st} = m_{dr}/3\pi\rho\nu d$  is the Stokes time,  $m_{dr} = (\pi/6) \rho_m d^3$  is the droplet mass, and  $\rho_m \gg \rho$  is the droplet mass density. The ratio,  $St = \tau_{st}/\tau_\eta = \rho_m d^2/18\rho \ell_\eta^2$ , of the Stokes time and the Kolmogorov turbulent turnover time,  $\tau_\eta$ , is the Stokes number, where  $\tau_\eta = \ell_\eta/u_\eta = \tau_0/\text{Re}^{1/2}$ ,  $u_\eta = u_0/\text{Re}^{1/4}$  is the characteristic velocity of eddies in the Kolmogorov micro-scale,  $\ell_\eta = \ell_0/\text{Re}^{3/4}$ ,  $\text{Re} = u_0\ell_0/\nu$  is the Reynolds number,  $u_0$  is the characteristic turbulent velocity in the integral turbulent scale  $\ell_0$  and  $\tau_0 = \ell_0/u_0$  is the turbulent time in the integral turbulent scale.

Solution of Eq. (3) for  $St \ll 1$  reads (see, e.g., Ref. 30):

$$\mathbf{v} = \mathbf{u} - \tau_{st} \left[ \frac{\partial \mathbf{u}}{\partial t} + (\mathbf{u} \cdot \nabla) \mathbf{u} - \mathbf{g} \right] + O(\tau_{st}^2). \quad (4)$$

This equation implies that  $\nabla \cdot \mathbf{v} \neq 0$ , i.e., the droplet velocity field is compressible,

$$\nabla \cdot \mathbf{v} = \nabla \cdot \mathbf{u} - \tau_{st} \nabla \cdot \left( \frac{d\mathbf{u}}{dt} \right) + O(\tau_{st}^2) = -\frac{1}{\rho} (\mathbf{u} \cdot \nabla) \rho + \frac{\tau_{st}}{\rho} \nabla^2 p + O(\tau_{st}^2), \quad (5)$$

In derivation of Eq. (5) we used the Navier-Stokes equation for the fluid. The mechanism of the clustering instability is associated with the droplet inertia. The centrifugal forces cause the droplets inside the turbulent eddies drift out to the boundary between the eddies, i.e., to the regions with the maximum fluid pressure fluctuations. Indeed, for a large Peclet number, when the molecular diffusion of droplets in Eq. (1) can be neglected, we can estimate  $dn/dt \propto -\nabla \cdot \mathbf{v}$ . Since  $\nabla \cdot \mathbf{v} \propto (\tau_{st}/\rho) \nabla^2 p \neq 0$  even for incompressible fluid, this implies that  $dn/dt \propto -(\tau_{st}/\rho) \nabla^2 p > 0$  in the regions where  $\nabla^2 p < 0$ . Therefore, the droplets are accumulated in regions with maximum pressure fluctuations.

## B. Mechanism of tangling clustering instability

In a case of temperature stratified turbulence with a non-zero large-scale temperature gradient, the turbulent heat flux  $\langle \mathbf{u} \theta \rangle$  is not zero. This implies correlation between fluctuations of fluid temperature,  $\theta$ , and velocity, and, therefore, the correlation between fluctuations of pressure and fluid velocity. In a temperature stratified turbulence there are additional pressure fluctuations caused by the tangling of the mean temperature gradient by the velocity fluctuations. This causes the increase of pressure fluctuations, and correspondingly enhance the droplet clustering.

Fluctuations of the droplet number density are described by the two-point second-order correlation function,  $\Phi(t, \mathbf{R}) = \langle n'(t, \mathbf{x}) n'(t, \mathbf{x} + \mathbf{R}) \rangle$ . The analysis of the tangling clustering instability employs the equation for the correlation function  $\Phi(t, \mathbf{R})$  that has been derived using the path-integral approach for random compressible flow with a finite correlation time (see Ref. 12):

$$\frac{\partial \Phi}{\partial t} = \left[ B(\mathbf{R}) - \frac{2}{\tau_{ev}} + 2\mathbf{U}^{(A)}(\mathbf{R}) \cdot \nabla + \hat{D}_{ij}(\mathbf{R}) \nabla_i \nabla_j \right] \Phi(t, \mathbf{R}), \quad (6)$$

where  $\mathbf{U}^{(A)}(\mathbf{R}) = (1/2) [\mathbf{U}(\mathbf{R}) - \mathbf{U}(-\mathbf{R})]$ ,

$$B(\mathbf{R}) \approx 2 \int_0^\infty \langle b[0, \boldsymbol{\xi}(t, \mathbf{x}|0)] b[\tau, \boldsymbol{\xi}(t, \mathbf{x} + \mathbf{R}|\tau)] \rangle d\tau, \quad (7)$$

$$U_i(\mathbf{R}) \approx -2 \int_0^\infty \langle v_i[0, \boldsymbol{\xi}(t, \mathbf{x}|0)] b[\tau, \boldsymbol{\xi}(t, \mathbf{x} + \mathbf{R}|\tau)] \rangle d\tau, \quad (8)$$

$$\hat{D}_{ij} = 2D_m \delta_{ij} + D_{ij}^T(0) - D_{ij}^T(\mathbf{R}), \quad (9)$$

$$D_{ij}^T(\mathbf{R}) \approx 2 \int_0^\infty \langle v_i[0, \boldsymbol{\xi}(t, \mathbf{x}|0)] v_j[\tau, \boldsymbol{\xi}(t, \mathbf{x} + \mathbf{R}|\tau)] \rangle d\tau. \quad (10)$$

The function  $B(\mathbf{R})$  is determined by the compressibility of the droplet velocity field,  $b = \text{div } \mathbf{v}$ . The vector  $\mathbf{U}(\mathbf{R})$  determines a scale-dependent drift velocity which describes transport of fluctuations of droplet number density from smaller scales to larger scales. The tensor of the scale-dependent turbulent diffusion  $D_{ij}^T(\mathbf{R})$  tends to the tensor of the molecular (Brownian) diffusion at very small scales, while in the vicinity of the integral turbulent scale it coincides with the tensor of turbulent diffusion. Other variables in Eqs. (6)-(10) are defined as follows:  $\delta_{ij}$  is the Kronecker tensor, the Wiener trajectory  $\boldsymbol{\xi}(t, \mathbf{x}|s)$  in the expressions for the turbulent diffusion tensor  $D_{ij}^T(\mathbf{R})$  and other transport coefficients is:  $\boldsymbol{\xi}(t, \mathbf{x}|s) = \mathbf{x} - \int_s^t \mathbf{v}[\tau, \boldsymbol{\xi}(t, \mathbf{x}|\tau)] d\tau + \sqrt{2D_m} \mathbf{w}(t - s)$ , and  $\langle \dots \rangle$  denotes averaging over the statistics of turbulent velocity field and the Wiener random process  $\mathbf{w}(t)$  that describes the

Brownian motion. The second term in the right hand side of Eq. (6) describes the effect of droplets evaporation.

The exponential growth of the correlation function of the droplet number density fluctuations,  $\Phi(t, \mathbf{R})$ , due to the tangling clustering instability, is determined by the first term,  $B(\mathbf{R}) \Phi(t, \mathbf{R})$ , in the right hand side of Eq. (6), which is the only positive one. To estimate the function  $B(\mathbf{R})$  we take into account the equation of state of an ideal gas that yields:  $p/P = \varrho/\rho + \theta/T + O(\varrho\theta/\rho T)$ , where  $\rho, T, P$  and  $\varrho, \theta, p$  are the mean and fluctuations of the fluid density, temperature, and pressure, respectively. For small Stokes numbers,  $\nabla \cdot \mathbf{v} \approx (\tau_{\text{st}}/\rho) \nabla^2 p + O(\text{St}^2)$ , we obtain

$$B(\mathbf{R}) \approx \frac{2\tau_{\text{st}}^2}{\rho^2} \langle \tau [\nabla^2 p(\mathbf{x})] [\nabla^2 p(\mathbf{y})] \rangle \approx \frac{2\tau_{\text{st}}^2}{\rho^2} \frac{P^2}{T^2} \langle \tau [\nabla^2 \theta(\mathbf{x})] [\nabla^2 \theta(\mathbf{y})] \rangle, \quad (11)$$

where  $\tau$  is the turbulent time. In  $\mathbf{k}$ -space the correlation function  $\langle \tau [\nabla^2 \theta(\mathbf{x})] [\nabla^2 \theta(\mathbf{y})] \rangle = \int \tilde{\tau}(k) k^4 \langle \theta(\mathbf{k}) \theta(-\mathbf{k}) \rangle \exp(i\mathbf{k} \cdot \mathbf{R}) d\mathbf{k}$ . Taking into account that the correlation function of temperature fluctuations,  $\langle \theta(\mathbf{k}) \theta(-\mathbf{k}) \rangle = \langle \theta^2 \rangle \tilde{E}_\theta(k)/4\pi k^2$ , and integrating in  $\mathbf{k}$ -space we obtain:

$$B(\mathbf{R}) \approx \frac{2\text{St}^2 c_s^4}{3\tau_\eta u_0^4} \left( \frac{\ell_0 \nabla T}{T} \right)^2 \text{Re}^{1/2}, \quad (12)$$

where  $c_s$  is the sound speed,  $\tilde{E}_\theta(k) = (2/3) k_0^{-1} (k/k_0)^{-5/3}$  is the spectrum function of the temperature fluctuations for  $k_0 \leq k \leq \ell_\eta^{-1}$ , with  $k_0 = \ell_0^{-1}$  and  $\tilde{\tau}(k) = 2\tau_0 (k/k_0)^{-2/3}$ . To determine  $\langle \theta^2 \rangle = 2E_\theta$  we used the budget equation for the temperature fluctuations:  $DE_\theta/Dt + \text{div } \Phi_\theta = -(\mathbf{F} \cdot \nabla)T - \varepsilon_\theta$ , that for homogeneous turbulence in a steady state yields:  $\langle \theta^2 \rangle = -2\tau_0 (\mathbf{F} \cdot \nabla)T = (2/3) (\ell_0 \nabla T)^2$ , where  $F_i = \langle u_i \theta \rangle = -D_T^{(\theta)} \nabla_i T$  is the turbulent heat flux,  $D_T^{(\theta)} = u_0 \ell_0 / 3$  is the coefficient of the turbulent diffusion of the temperature fluctuations and the dissipation rate of  $E_\theta$  is  $\varepsilon_\theta = \langle \theta^2 \rangle / 2\tau_0$ .

In a non-stratified turbulence ( $\nabla T = 0$ ), the function  $B(\mathbf{R}) = 20\sigma_v/\tau_\eta(1 + \sigma_v)$ , where  $\sigma_v \equiv \langle (\nabla \cdot \mathbf{v})^2 \rangle / \langle (\nabla \times \mathbf{v})^2 \rangle$  is the degree of compressibility of the particle velocity field. For small Stokes numbers,  $\sigma_v \approx (8/3)\text{St}^2$ , so that  $B(\mathbf{R}) = 160\text{St}^2/3\tau_\eta$ . (for details see Refs. 12). Therefore, in general case that includes both, the tangling clustering instability and the inertial clustering instability, the function  $B(\mathbf{R})$  can be written in the following form (see Ref. 29):

$$B(\mathbf{R}) = \frac{160\text{St}^2 \Gamma^2}{3\tau_\eta}, \quad \Gamma(\text{Ma}, \text{Re}, \ell_0/L_T) = \left[ 1 + \frac{\text{Re}^{1/2}}{81\text{Ma}^4} \left( \frac{\ell_0 \nabla T}{T} \right)^2 \right]^{1/2}. \quad (13)$$

Here  $L_T = T/|\nabla T|$  is the characteristic scale of the mean temperature variations and we took into account that for a Gaussian velocity field:  $\langle(\nabla \cdot \mathbf{v})^2\rangle = (80/3\tau_\eta^2)\text{St}^2\Gamma^2$  and  $\langle(\nabla \times \mathbf{v})^2\rangle = 10/\tau_\eta^2$ . For typical parameters of atmospheric turbulence:  $\text{Re} = 10^6 - 10^7$ ,  $u_0 = (0.5 - 1)$  m/s,  $\ell_0 = 100$  m and the mean temperature gradient,  $|\nabla T| = 1$  K / 100 m, the dimensionless parameter  $\Gamma = (3 - 20) \times 10^3$ . The inertial clustering instability corresponds to the case of  $\Gamma = 1$ .

As follows from Eq. (13), the temperature fluctuations, which are caused by the tangling of the mean temperature gradient,  $\nabla T$ , by the fluid velocity fluctuations  $\mathbf{u}$ , strongly contribute to the function  $B(\mathbf{R})$  and the growth rate of the tangling clustering instability in the temperature-stratified turbulence. The mechanism of coupling related to the tangling of the gradient of the mean temperature gradient is quite robust. The tangling is not sensitive to the exponent of the energy spectrum of the background turbulence. Anisotropy effects do not introduce new physics in the clustering process because the main contribution to the tangling clustering instability is at the Kolmogorov (viscous) scale of turbulent motions, where turbulence can be considered as nearly isotropic, while anisotropy effects can be essential in the vicinity of the maximum scales of the turbulent motions.

Equation (13) shows that the tangling clustering instability can be much more effective than the inertial clustering instability which is excited in a non-stratified turbulence (see Ref. 12). In both instabilities, the particle clustering is determined by the two-point correlation function of the Laplacian of air pressure fluctuations. However, in case of non-stratified turbulence the pressure fluctuations are of the order of  $\rho\mathbf{u}^2$ , while in case of the temperature-stratified turbulence there are additional pressure fluctuations caused by temperature fluctuations,  $p \propto P(\theta/T) \propto \rho c_s^2(\theta/T)$ . Consequently, the ratio of the two-point correlation functions of the Laplacian of air pressure fluctuations in stratified and non-stratified flows is proportional to  $(\theta/T)^2/\text{Ma}^4$ , which is a very large parameter for low Mach numbers (e.g., in the atmospheric turbulence  $\text{Ma} = u_0/c_s = 10^{-3}$ ).

In this study we consider low-Mach number compressible flow of the ideal gas. For temperature stratified turbulence the turbulent heat flux does not vanish, the fluctuations of air temperature are correlated with the fluctuations of velocity and, correspondingly, with fluctuations of pressure. In the limiting case of the incompressible fluid the effect of temperature stratification vanishes. Due to inertia effects droplets accumulate in the regions with the increased pressure of the air flow. The effect of increased pressure fluctuations in a

temperature stratified turbulence is more effective in small scales because the function  $B(\mathbf{R})$  is determined by the two-point correlation function of the Laplacian of pressure fluctuations.

The tangling clustering is also enhanced by the effect of turbulent thermal diffusion (see Ref. 35) that causes non-diffusive streaming of particles in the direction of a heat flux and accumulation of particles in the regions with the minimum mean temperature of the air flow. Temperature fluctuations in the stratified turbulence produce pressure fluctuations and cause particle clustering due to the tangling clustering instability with the growth rate, that is by a factor  $\sqrt{\text{Re}} (\ell_0/L_T)^2 (3\text{Ma})^4$  larger than the growth rate of the inertial clustering instability [see Eq. (13)]. For large Reynolds numbers the tangling mechanism is universal and independent of the origin of turbulence.

### C. Growth rate of the instability

To illustrate the tangling clustering instability we use the standard dependence of the droplet evaporation time on their diameter and the relative humidity [see Eq. (18) below]. Figure 1 shows the growth rate of the instability (measured in the inverse turbulent Kolmogorov time scale units,  $\tau_\eta^{-1}$ ) versus the droplet diameter  $d$  (measured in  $\mu\text{m}$ ) for different values of relative humidity,  $\phi$ , i.e., for very low humidity (45% and 85%) and for very high humidity (99.8% and 100%). Inspection of Fig. 1 shows that there is a sharp maximum of the growth rate for  $d = 1.7 - 1.8 \mu\text{m}$  if the relative humidity is close to saturation, 99.8% and 100%. This explains the fast growth of the droplets having the initial diameter of the order of  $2 \mu\text{m}$  caused by the tangling clustering instability. For lower values of the relative humidity the droplet growth rate sharply decreases.

The exponential growth of droplet number density inside the cluster is saturated by non-linear effects. The droplet number density inside the cluster can be constraint by depletion of particles in the surrounding air flow caused by their accumulation inside the cluster. Another effect that inhibits the growth of the droplet number density inside the cluster is related to a strong momentum coupling of particles and turbulent air flow when the mass loading parameter  $m_{\text{dr}} n_{\text{max}}/\rho \approx 0.5$ . It can be shown (see Ref. 29) that the maximum increase of particle number density inside the cluster,  $n_{\text{max}}/N$ , caused by the first effect is:

$$\frac{n_{\text{max}}}{N} = \left( 1 + \frac{e \lambda}{\pi} \text{Sc}^{\lambda/2} \ln \text{Sc} \right)^{1/2}, \quad (14)$$

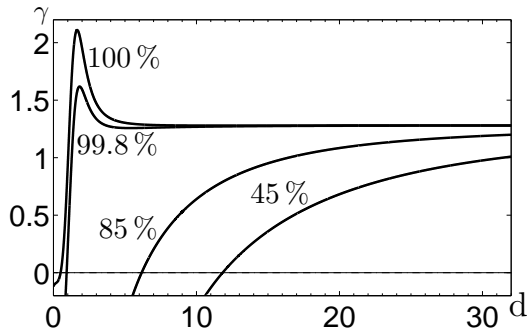


FIG. 1. Growth rate  $\gamma$  of the tangling clustering instability (measured in units  $1/\tau_\eta$ ) versus the droplet diameter  $d$  (measured in  $\mu\text{m}$ ) for  $\Gamma = 10^4$  and  $\text{Sc} = 5 \times 10^5 d$ .

where  $\text{Sc} = \nu/D_m$  is the Schmidt number. In this analysis small yet finite molecular diffusion  $D_m$  has been taken into account. For instance, the Schmidt number for droplets in the atmospheric flow is  $\text{Sc} = 0.7 \times 10^6 d(m\mu)$ . It should be noted that in the limit  $D_m = 0$  Eq. (14) is not valid. Parameter  $\lambda(\sigma_v) = (20\sigma_v + 1)/4(\sigma_v + 1)$  in Eq. (14) depends on the degree of compressibility of the particle velocity field,  $\sigma_v \approx \text{St}^2 \Gamma$ . For typical parameters of atmospheric turbulence, parameter  $\lambda$  varies in the range from 0.5 to 2.5.

Let us estimate the limitation caused by strong momentum coupling of particles and turbulent air flow. Assuming a total cloud water content  $\bar{\rho}_{\text{dr}} \equiv m_{\text{dr}} n_{\text{max}} = 1.5 \text{ g/m}^3$  and taking into account that the air density in the atmosphere  $\rho \approx 1.3 \times 10^3 \text{ g/m}^3$ , we obtain:  $n_{\text{max}}/N < 0.5 \rho/\bar{\rho}_{\text{dr}} \approx 470$ . Figure 2 shows the increase of droplets concentration  $n_{\text{max}}/N$  inside the cluster during development of the tangling clustering instability for the relative humidity 99.8 % and 100 %. The growth rate of the instability is of the order of 10 inverse Kolmogorov time-scales, where  $\tau_\eta \approx 0.1 \text{ s}$ .

Note that at the initial stage of the tangling clustering instability, the increase of the droplet number density in the cluster for small droplets  $d < 1 \mu\text{m}$  is not as effective as for larger droplets. It must be also noted that in this study we consider only droplet clustering, but not aerosol dynamics. Clearly, the clustering of aerosols is similar to that of droplets for humidity of 100 %, i.e. without evaporation.

The experimental study of the particle clustering in a temperature stratified turbulence have been reported in Ref. 31. The experimental parameters were: the r.m.s. velocity  $u_0 = 12 \text{ cm/s}$ , the integral (maximum) scale of turbulence  $\ell_0 = 3.2 \text{ cm}$ , the Reynolds

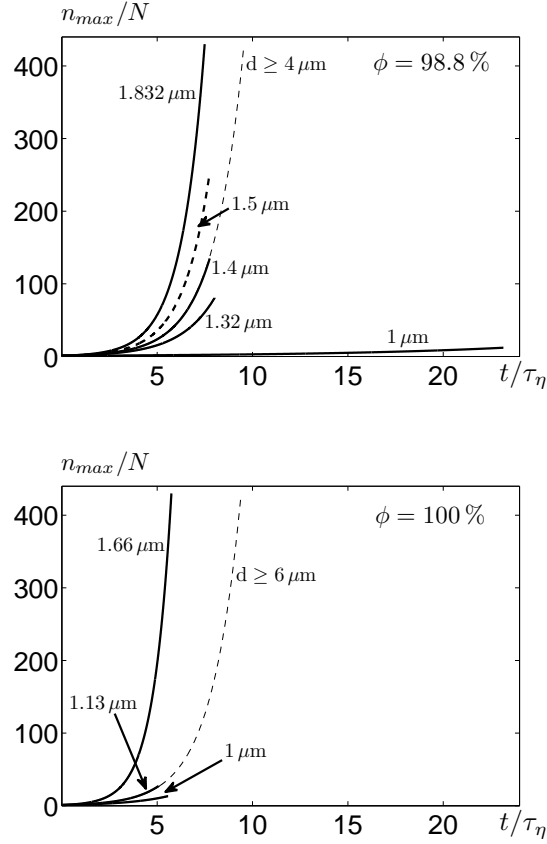


FIG. 2. The time evolution of droplet concentration  $n_{\max}/N$  inside the cluster for droplets of different diameter for relative humidity 99.8 % (upper panel) and 100 % (bottom panel);  $\Gamma = 10^4$  and  $\text{Sc} = 5 \times 10^5 d$ .

numbers  $\text{Re} = 250$ , the Kolmogorov length scale  $\ell_\eta = 510 \mu\text{m}$  and the Kolmogorov time scale  $\tau_\eta = 1.7 \times 10^{-2}$  s. The Stokes time for the particles with the diameter  $d = 10 \mu\text{m}$  is  $\tau_{\text{st}} = 10^{-3}$  s, the Stokes number  $\text{St} = 5.9 \times 10^{-2}$ , the coefficient of molecular diffusion  $D_m = 1.4 \times 10^{-8}$   $\text{cm}^2/\text{s}$  and the Peclet number  $\text{Pe} = u_0 \ell_0 / D_m = 3 \times 10^9$ . These experiments demonstrated that the two-point correlation function of the particle number density fluctuations for the tangling clustering in temperature stratified turbulence is by one order of magnitude larger than that for the inertial clustering in isothermal turbulence. Measured correlation functions of the particle number density fluctuations in temperature stratified turbulence were found in a good agreement with that predicted by the theory.

### III. COLLISION KERNEL AND DROPLET COAGULATION

In this Section we consider droplet coagulation and apply the theory of the tangling clustering instability to explain acceleration of raindrops formation in warm clouds. The warm clouds often exist in the region of atmospheric turbulent convection with coherent structures (cloud “cells” in shear-free convection and cloud “streets” in sheared convection, see e.g., Refs. 36 and 37). The vertical large-scale temperature gradient is small inside the large-scale circulation (coherent structures) in a small-scale turbulent convection. However, the horizontal large-scale temperature gradient inside the circulations is not small. Atmospheric observations showed that this gradient is about 1 K per 100 m (see Ref. 38). Similar results were reported in laboratory experiments where the horizontal large-scale temperature gradient inside the large-scale circulation was 0.6 K per 1 cm, while the vertical large-scale temperature gradient was 0.05 K per 1 cm (see Ref. 39). This magnitude of the horizontal temperature gradient is sufficient for the generation of strong temperature fluctuations in the stratified turbulence by tangling mechanism.

The initial stage of cloud droplets formation involves condensation of water vapor on cloud condensation nuclei (CCN) and formation of small micron size droplets. In the present study we show that the tangling clustering instability strongly enhances the growth rate of cloud droplets at both stages: at the first stage when droplets grow from the micron size to 10  $\mu\text{m}$  droplets and at the next stage from 10 to 50  $\mu\text{m}$  radius droplets.

#### A. Smoluchowski coagulation equation

Subsequent evolution and growth of small droplets due to collision-coalescence depend on the interplay between their collision time and evaporation time, in particular because of water vapor depletion. The collision time of small droplets can be determined using the Smoluchowski coagulation equation (see, e.g., Ref. 40, Chapter 13):

$$\frac{\partial \tilde{n}(d)}{\partial t} + \text{div}(\tilde{n} \mathbf{v}) - D_m \Delta \tilde{n} + \frac{\tilde{n}}{\tau_{ev}} = \frac{1}{2} \int_0^d K(\hat{d}, x) \tilde{n}(\hat{d}) \tilde{n}(x) dx - \int_0^\infty K(d, x) \tilde{n}(x) \tilde{n}(d) dx, \quad (15)$$

where  $\hat{d} = (d^3 - x^3)^{1/3}$ ,  $\tilde{n}(d)$  is the droplet size distribution,  $n = \int \tilde{n}(x) dx$  is number density of droplets, and  $K(d, x)$  is the coagulation kernel that describes coagulation rate of droplets of the diameter  $d$  and droplets of the diameter  $x$ . In the present study we use the coagulation

kernel  $K(d, x)$  as a sum of the Brownian coagulation kernel (see Table 13.1, p. 600 in Ref. 40) and the gravitational coagulation kernel (see Eq. (13.A.4), p. 615 in (see Ref. 40)).

Averaging Eq. (15) over the statistics of particle turbulent velocity field, estimating integrals in Eq. (15), using the mean-value theorem, and taking into account that  $\langle \tilde{n}(d) \tilde{n}(d_1) \rangle$  is calculated in the same point, so that  $\langle \tilde{n}(d) \tilde{n}(d_1) \rangle \leq \tilde{n}_{\max}(d) \tilde{n}_{\max}(d_1) = C(d, d_1) \tilde{N}(d) \tilde{N}(d_1)$ , we obtain the following equation for the mean droplet size distribution  $\tilde{N}(d)$ :

$$\frac{\partial \tilde{N}(d)}{\partial t} + \text{div} \left( \tilde{N} \mathbf{U} + \langle \tilde{n}' \mathbf{u} \rangle \right) = -\frac{\tilde{N}}{\tau_{\text{ev}}(d)} - \frac{\tilde{N}}{\tau_{\text{eff}}^{\text{st}}(d)} + D_T \Delta \tilde{N}, \quad (16)$$

where  $C(d, d_1) = \tilde{n}_{\max}(d) \tilde{n}_{\max}(d_1) / \tilde{N}(d) \tilde{N}(d_1)$ ,  $D_T(d)$  is the turbulent diffusion coefficient and

$$\tau_{\text{eff}}^{\text{st}}(d) = \frac{1}{\tilde{N}(d) K(d, d_1) C(d, d_1)} > \frac{1}{\tilde{N}(d) K(d, d_1)} \left( \frac{\tilde{n}_{\max}(d)}{\tilde{N}(d)} \right)^{-2}. \quad (17)$$

Notably, the collision term  $\tilde{N}(d)/\tau_{\text{eff}}^{\text{st}}(d)$  in Eq. (16) is similar to the droplet evaporation term. The coefficient of molecular diffusion of droplets having the diameter  $d$  in the atmosphere is  $D_m = 2 \times 10^{-7} / d(m\mu) \text{ cm}^2 \text{ s}^{-1}$ , while the turbulent diffusion coefficient  $D_T = u_0 \ell_0 / 3 = 3 \times 10^5 \text{ cm}^2 \text{ s}^{-1}$ , where turbulent velocity  $u_0$  at the integral turbulent scale  $\ell_0 = 100 \text{ m}$  is  $u_0 = 1 \text{ m/s}$ . Therefore, the coefficient of molecular diffusion of droplets is much smaller than the turbulent diffusion coefficient.

## B. Effective collision-coalescence time

Now we can estimate the droplet collision time and compare it with the evaporation time of droplets having different sizes. The most interesting case is the growth of droplets when the relative humidity is only slightly less 100% and the evaporation of droplets competes with their coagulation. Figure 3 shows the numerical values of the sum of the Brownian and gravitational coagulation kernels versus droplet diameter  $d$  when droplets have the same or different sizes (see Ref. 40). Inspection of Fig. 3 shows that the collision kernel varies slightly when  $d < 2 \mu\text{m}$ , and it increases by one order of magnitude for  $d = 5 \mu\text{m}$ , while for  $d > 5 \mu\text{m}$  the collision kernel can increase by three orders of magnitude depending on the difference in size of colliding droplets ( $d$  and  $d_1$ ). However, the effect of this increase on the droplet collision rate is much smaller than the increase of droplet collision rate due to increase of the droplet number density caused by the tangling clustering instability that is up to five orders of magnitude.

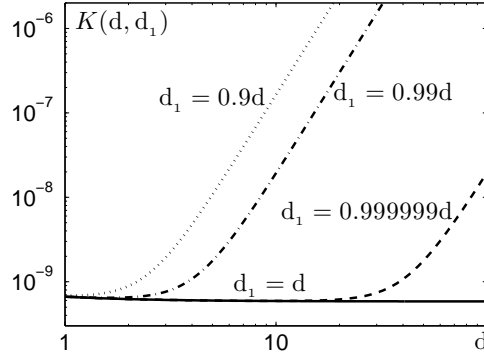


FIG. 3. Sum of Brownian and gravitational coagulation kernels versus the droplet diameter  $d$  in microns for two droplets having different diameters:  $d = 0.9d_1$  - dotted line;  $d = 0.99d_1$  - dashed-dotted line;  $d - d_1 = 10^{-6}d$  - dashed line. Solid line is Brownian coagulation kernel  $K(d, d_1)$  [measured in  $\text{cm}^3/\text{s}$ ] for two droplets having equal diameters  $d = d_1$ . The diameter  $d$  of droplets is measured in  $\mu\text{m}$ .

Dynamics of the raindrops evolution and their growth depend on the interplay between the characteristic times of droplet collisions resulting in droplet coagulation and the time of droplet evaporation. The characteristic times of vapor diffusion and thermal relaxation in the gaseous phase in the vicinity of a droplet can be estimated as  $\tau_{\text{dif}} \propto d^2/D_v$ , and  $\tau_{\text{th}} \propto d^2/\chi$ , where  $D_v = 0.216 \text{ cm}^2 \text{ s}^{-1}$  is coefficient of binary diffusion of water vapor in air and  $\chi = 0.185 \text{ cm}^2 \text{ s}^{-1}$  is thermal diffusivity of air (see Ref. 40). Since these characteristic times are much smaller than the time of droplet evaporation or growth, the evaporation/growth of cloud droplets is determined by stationary vapor diffusion. In this case the characteristic time of the decrease of droplet radius due to evaporation can be estimated using the coupled analytical model of the evaporation/growth rates of droplets (see Ref. 41). For the ambient air temperature  $T_a = 274 \text{ K}$ , this model yields the following expression for the evaporation time:

$$\tau_{\text{ev}} = 0.5 \times 10^{-3} \frac{d^2}{1 - \phi}, \quad (18)$$

where the droplet diameter is measured in microns and time is given in seconds. The calculated evaporation times versus droplet radius for relative humidity  $\phi = 99\%$  and  $\phi = 99.99\%$  together with the effective collision-coalescence time within the cluster are shown in Fig. 4. To determine the effective collision-coalescence time we have assumed that a

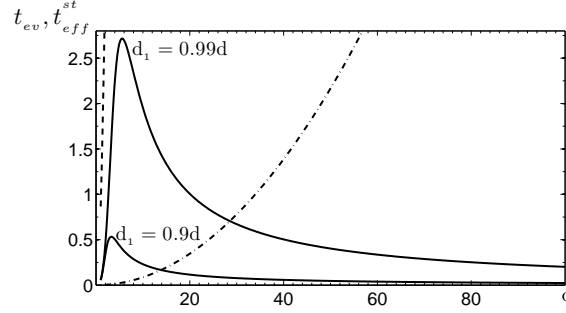


FIG. 4. Evaporation times versus droplet diameter for relative humidity  $\phi = 99\%$  (dashed-dotted line) and  $\phi = 99.99\%$  (dashed line) and effective collision-coalescence time (solid lines for different  $d - d_1$ ). The diameter  $d$  of droplets is measured in  $\mu\text{m}$  and time is measured in minutes.

total cloud water content of mean droplets mass density is about  $\bar{\rho}_{\text{dr}} = 1.5 \text{ g/m}^3$ , which corresponds to the typical mean number density of  $10 \mu\text{m}$  droplets,  $N \approx 2 \text{ cm}^{-3}$ , while for  $2 \mu\text{m}$  droplets it is about  $N \approx 2 \times 10^2 \text{ cm}^{-3}$ .

In the absence of tangling clustering instability, for the ambient number density of the micron size droplets having the mean number density  $N \approx 10^2 \text{ cm}^{-3}$ , the collision-coalescence time is of the order of  $\tau_{\text{eff}}^{\text{st}}(d = 2 \mu\text{m}) \approx (\tilde{N} K)^{-1} \approx 10^7 \text{ s}$ , and for droplets with diameter  $d = 10 \mu\text{m}$  and the mean number density  $N(d = 10 \mu\text{m}) \approx 1 \text{ cm}^{-3}$ , the collision-coalescence time is  $\tau_{\text{eff}}^{\text{st}}(d = 10 \mu\text{m}) > 10^7 \text{ s}$ . These values are too large to account for the collision-coalescence growth of cloud droplets since the droplet evaporation time is much less than their collision time. The latter conclusion implies that small micron-size and submicron-size droplets are either in equilibrium or grow very slowly due to condensation of supersaturated water vapor. In these calculations we have taken into account kinetic corrections to submicron-size droplet evaporation time using the flux-matching approach suggested in Ref. 42.

The situation drastically changes in the presence of the tangling clustering instability. In this case the droplet collision time inside the clusters, which are formed due to the tangling clustering instability, decreases by the large factor,  $[n_{\text{max}}/N]^2 \sim 10^5$ . Indeed, the number density of droplets inside the cluster sharply increases and their effective collision time dramatically decreases:

$$\tau_{\text{eff}}^{\text{st}} = \frac{1}{\tilde{N}(d) K(d, d_1)} \left( \frac{n_{\text{max}}}{N} \right)^{-2}. \quad (19)$$

Using the numerical values of the coagulation kernel showed in Fig. 3 we can estimate the

effective collision-coalescence time inside the cluster. The equilibrium between the effective droplet collision-coalescence and droplet evaporation depends on the value of the relative humidity  $\phi$  and the temperature of the ambient air. The calculated effective collision times inside the cluster for two typical values of the relative humidity for  $T = 274$  K versus the droplet diameter are shown by solid lines in Fig. 4.

Using data shown in Fig. 4, we estimate the time of growth of droplets by cascade of successive collisions of droplets having close diameters (with diameters ratios  $d_1/d = 1.1$  or  $d_1/d = 1.01$ ). In the calculations we take into account that after each collision droplet diameter increases, and effective droplet collision time changes non-monotonically as shown in Fig. 4. For  $d_1/d = 1.1$  the time of droplet size growth from  $1 \mu\text{m}$  to  $10 \mu\text{m}$  diameter is about 3 minutes, while for  $d_1/d = 1.01$  this time is approximately 11 minutes. The time required for further droplet size growth from  $10 \mu\text{m}$  to  $(50 - 60) \mu\text{m}$  diameter droplets is about 1 min for  $d_1/d = 1.1$  and 5.5 minutes for colliding droplets diameters ratio  $d_1/d = 1.01$ . It should be noted that real droplet size growth time can be shorter due to direct enhancement of droplet collision kernel by turbulence (see Ref. 1 and references therein). Since droplet collisional growth time is smaller for droplets with larger diameters ratios, the estimated droplet growth time can be considered as a fairly reasonable estimate of the time required for droplet growth. The total time required for collisional growth of droplets having diameter  $1 \mu\text{m}$  to droplets having diameter about  $50 \mu\text{m}$  is of the order of 15 minutes that is close to the observed  $(15 - 20)$  minutes required for formation of rain droplets.

#### IV. CONCLUSIONS

New effect of the tangling clustering instability of small droplets in turbulent temperature stratified atmosphere results in the formation of clusters with drastically increased droplet number density and, correspondingly, sharply increased rate of their collision-coalescence. Without the tangling clustering instability, the droplets collision-coalescence time is much larger than the characteristic time of the droplet evaporation. Consequently, in the absence of tangling clustering instability droplets do not grow due to collision-coalescence, and rain droplets are not formed. On the contrary, in the presence of tangling clustering instability the effective collision-coalescence time inside the clusters strongly decreases by the factor  $[n_{\text{max}}/N]^2 \sim 10^5$ . As the result, droplets within the cluster coalesce and grow forming large

rain droplets. The growth time of droplets from the initial size of  $1\ \mu\text{m}$  up to the size of about  $50\ \mu\text{m}$  is 15 – 20 minutes.

*In summary*, we can conclude that the effect of the tangling clustering instability provides a convincing explanation of the observed fast growth of cloud droplets.

## ACKNOWLEDGMENTS

This work has been supported by the Israel Science Foundation governed by the Israeli Academy of Sciences (grant No. 1037/11); COST ES1004; EC FP7 project ERC PBL-PMES (grant 227915), the Research Council of Norway under the FRINATEK (grant No. 231444), Russian-Government mega grant (No. 11.G34.31.0048), and grant of Russian Ministry of Science and Education (Program 1.5/XX, contract No. 8648).

## REFERENCES

- <sup>1</sup>A. Khain, M. Pinsky, T. Elperin, N. Kleorin, I. Rogachevskii and A. Kostinski, “Critical comments to results of investigations of drop collisions in turbulent clouds,” *Atmosph. Res.* **86**, 1 (2007).
- <sup>2</sup>B. J. Devenish, P. Bartello, J.-L. Brenguier, L. R. Collins, et al., “Droplet growth in warm turbulent clouds. Review Article,” *Q. J. R. Meteorol. Soc.* **138**, 1401 (2012).
- <sup>3</sup>W. W. Grabowski and L-P. Wang, “Growth of Cloud Droplets in a Turbulent Environment,” *Annu. Rev. Fluid Mech.* **45**, 293 (2013).
- <sup>4</sup>H. R. Pruppacher and J. D. Klett, *Microphysics of Clouds and Precipitation*, 2nd ed. (Kluwer Academic, Dordrecht, 1997).
- <sup>5</sup>A. M. Blyth, S. G. Lasher-Trapp, W. A. Cooper, C. A. Knight and J. Latham, “The role of giant and ultragiant nuclei in the formation of early radar echoes in warm cumulus clouds,” *J. Atmos. Sci.* **60**, 2557 (2003).
- <sup>6</sup>P. A. Vaillancourt, M. K. Yau and W. W. Grabowski, “Microscopic approach to cloud droplet growth by condensation. Part I: Model description and results without turbulence,” *J. Atmos. Sci.* **58**, 1945 (2001).
- <sup>7</sup>P. A. Vaillancourt, M. K. Yau, P. Bartello and W. W. Grabowski, “Microscopic approach to cloud droplet growth by condensation. Part II: Turbulence, clustering, and condensational

- growth,” *J. Atmos. Sci.* **59**, 3421 (2002).
- <sup>8</sup>P. Tisler, E. Zapadinsky and M. Kulmala, “Initiation of rain by turbulence-induced condensational growth of cloud droplets,” *Geophys. Res. Lett.* **32**, L06806 (2005).
- <sup>9</sup>L.-P. Wang, A. Orlando, B. Rosa and W. W. Grabowski, “Turbulent collision efficiency of heavy particles relevant to cloud droplets, *New J. Phys.* **10**, 075013 (2008).
- <sup>10</sup>L.-P. Wang and M. R. Maxey, “Settling velocity and concentration distribution of heavy particles in homogeneous isotropic turbulence,” *J. Fluid Mech.* **256**, 27 (1993).
- <sup>11</sup>T. Elperin, N. Kleorin, I. Rogachevskii, “Self-excitation of fluctuations of inertial particles concentration in turbulent fluid flow,” *Phys. Rev. Lett.* **77**, 5373 (1996).
- <sup>12</sup>T. Elperin, N. Kleorin, V. L’vov, I. Rogachevskii, D. Sokoloff, “Clustering instability of the spatial distribution of inertial particles in turbulent flows,” *Phys. Rev. E* **66**, 036302 (2002).
- <sup>13</sup>T. Elperin, N. Kleorin, M.A. Liberman, V.S. L’vov, I. Rogachevskii, “Clustering of aerosols in atmospheric turbulent flow,” *Environ. Fluid Mech.* **7**, 173 (2007).
- <sup>14</sup>M. B. Pinsky and A. P. Khain, “Turbulence effects on droplet growth and size distribution in clouds. A review,” *J. Aerosol Sci.* **28**, 1177 (1997).
- <sup>15</sup>M. B. Pinsky and A. P. Khain, “Formation of inhomogeneity in drop concentration induced by drop inertia and their contribution to the drop spectral broadening,” *Quart. J. Roy. Meteor. Soc.* **123**, 165 (1997).
- <sup>16</sup>M. B. Pinsky and A. P. Khain, “Effects of in-cloud nucleation and turbulence on droplet spectrum formation in cumulus clouds, *Quart. J. Roy. Meteor. Soc.* **128**, 501 (2002).
- <sup>17</sup>M. B. Pinsky and A. P. Khain, “Collisions of small drops in a turbulent flow. Part II: Effects of flow accelerations,” *J. Atmos. Sci.* **61**, 1926 (2004).
- <sup>18</sup>L.-P. Wang, A. S. Wexler and Y. Zhou, “Statistical mechanical descriptions of turbulent coagulation of inertial particles,” *J. Fluid Mech.* **415**, 117 (2000).
- <sup>19</sup>L.-P. Wang, O. Ayala, S. E. Kasprzak and W. W. Grabowski, “Theoretical formulation of collision rate and collision efficiency of hydrodynamically interacting cloud droplets in turbulent atmosphere,” *J. Atmos. Sci.* **62**, 2433 (2005).
- <sup>20</sup>Y. Zhou, A. S. Wexler and L.-P. Wang, “Modelling turbulent collision of bidisperse inertial particles,” *J. Fluid Mech.*, **433**, 77 (2001).
- <sup>21</sup>J. Davila and J. C. R. Hunt, “Settling of small particles near vortices and in turbulence,” *J. Fluid Mech.* **440**, 117 (2001).

- <sup>22</sup>Z. Dodin and T. Elperin, “On the collision rate of particles in turbulent flow with gravity,” *Phys. Fluids* **14**, 2921 (2002).
- <sup>23</sup>G. Falkovich, A. Fouxon and M. G. Stepanov, “Acceleration of rain initiation by cloud turbulence,” *Nature* **419**, 151 (2002).
- <sup>24</sup>S. Ghosh, J. Davila, J. C. R. Hunt, A. Srdic, H. J. S. Fernando and P. Jonas, “How turbulence enhances coalescence of settling particles with applications to rain in clouds,” *Proc. Roy. Soc. London* **461** A, 3059 (2005).
- <sup>25</sup>K. D. Squires and J. K. Eaton, “Preferential concentration of particles by turbulence,” *Phys. Fluids* **A3**, 1169 (1991).
- <sup>26</sup>M. Gavaises, A. Theodorakakos, G. Bergeles, and G. Breen, “Evaluation of the effect of droplet collisions on spray mixing,” *Proc. Inst. Mech. Eng.* **210**, 465 (1996).
- <sup>27</sup>P. Villedieu and O. Simonin, “Modeling of coalescence in turbulent gas-droplet flows,” *Comm. Math. Sci., Suppl. issue* **1**, 13 (2004).
- <sup>28</sup>C. Tang, P. Zhang and C. K. Law, “Bouncing, coalescence, and separation in head-on collision of unequal-size droplets,” *Phys. Fluids* **24**, 022101 (2012).
- <sup>29</sup>T. Elperin, N. Kleorin, M. A. Liberman and I. Rogachevskii, “Tangling clustering instability for small particles in temperature stratified turbulence,” *Phys. Fluids* **25**, 085104 (2013).
- <sup>30</sup>M. R. Maxey, “The gravitational settling of aerosol particles in homogeneous turbulence and random flow field,” *J. Fluid Mech.* **174**, 441 (1987).
- <sup>31</sup>A. Eidelman, T. Elperin, N. Kleorin, B. Melnik and I. Rogachevskii, “Tangling clustering of inertial particles in stably stratified turbulence,” *Phys. Rev. E* **81**, 056313 (2010).
- <sup>32</sup>J. Eggers, “Nonlinear dynamics and breakup of free surface flows,” *Rev. Mod. Phys.* **69**, 865 (1997).
- <sup>33</sup>J. Eggers, J. R. Lister and H. A. Stone, “Coalescence of liquid drops,” *J. Fluid Mech.* **401**, 293 (1999).
- <sup>34</sup>L. Duchemin, J. Eggers and C. Josserand, “Inviscid coalescence of drops,” *J. Fluid Mech.* **487**, 167 (2003).
- <sup>35</sup>T. Elperin, N. Kleorin and I. Rogachevskii, “Turbulent thermal diffusion of small inertial particles,” *Phys. Rev. Lett.* **76**, 224 (1996).
- <sup>36</sup>D. Etling and R. A. Brown, “Roll vortices in the planetary boundary layer: a review,” *Boundary-Layer Meteorol.* **65**, 215 (1993).

- <sup>37</sup>B. W. Atkinson and J. Wu Zhang, “Mesoscale shallow convection in the atmosphere,” *Rev. Geophys.* **34**, 403 (1996).
- <sup>38</sup>A. G. Williams and J. M. Hacker, “The composite shape and structure of coherent eddies in the convective boundary layer,” *Boundary-Layer Meteorol.* **61**, 213 (1992).
- <sup>39</sup>M. Bukai, A. Eidelman, T. Elperin, N. Kleerorin, I. Rogachevskii and I. Sapir-Katiraie, “Effect of large-scale coherent structures on turbulent convection,” *Phys. Rev. E* **79**, 066302 (2009).
- <sup>40</sup>J. H. Seinfeld and S. N. Pandis, *Atmospheric Chemistry and Physics. From Air Pollution to Climate Change.*, 2nd ed. (John Wiley & Sons, NY, 2006).
- <sup>41</sup>A. B. Nadykto, E. R. Shchukin, M. Kulmala, K. E. J. Lehtinen and A. Laaksonen, “Evaporation and Condensational Growth of Liquid Droplets in Nonisothermal Gas Mixtures,” *Aerosol Science and Technology* **37**, 315 (2003).
- <sup>42</sup>A. A. Lushnikov and M. Kulmala, “Flux-matching theory of particle charging,” *Phys. Rev. E* **70**, 046413 (2004).